Pergamon

Int. J. Heat Mass Transfer. Vol. 38, No. 7, pp. 1317–1325, 1995

0017–9310/95 $9.50+0.00

0017–9310(94)00234–7

A transient-state technique for the heat transfer coefficient measurement in a corrugated plate heat exchanger channel based on frequency response and residence time distribution

S. ROS, C. JALLUT,† J. M. GRILLOT and M. AMBLARD
GRETh–CENG, 17 rue des Martyrs, 38054 Grenoble cedex 9, France

(*Received* 18 *February* 1994 *and in final form* 11 *July* 1994)

Abstract—Transient techniques are widely used for the measurement of heat transfer coefficient in heat exchangers: using such methods generally leads to simplified experimental procedures. The measured coefficient is obtained by minimizing the distance between a model of the system and experimental data. In this paper, we use such a transient-state technique to measure the global heat exchange coefficient between a liquid and corrugated plates. The model usually employed in the heat exchangers area is based on the hypothesis that the fluid flow is similar to a plug flow. Axial dispersion is then considered by defining an apparent axial dispersion coefficient in the fluid and by considering axial or transversal heat conduction in the solid. We propose here to model the fluid flow by an equivalent flow pattern obtained by inert tracer experiments. Such a representation, similar to those used to model flows through chemical reactors, is then completed by the heat transfer model in the solid. In the latter, only transversal conduction is considered. The model that we derive is in fact similar to those used to model percolation processes through porous media. We give some experimental evidences based on pressure drop measurements that such a comparison is correct. The frequency response is then used to estimate the heat transfer coefficient between the fluid and the solid. The values obtained by this method are very close to that already known for such corrugated plates.

INTRODUCTION

Heat transfer between a fluid and a solid is a rather complicated phenomenon involving conduction in the solid as well as conduction and convection in the fluid. In order to describe precisely such a situation, one needs to solve simultaneously energy and momentum equations in the fluid and the energy equation in the solid. Consequently, heat transfer modelling in the fluid is often drastically simplified by defining a heat exchange coefficient h by reference to a given fluid temperature: in many practical applications, this sole coefficient is very useful [1]. Compared with the exact situation, one will frequently find that this coefficient varies according to time and space. For example, the problem of the time variation of h has been addressed in ref. [2]; h may also vary because of fluid physical property variations due to large temperature changes.

The measurement of such a global heat exchange coefficient is obtained from steady- or transient-state experiments. For example, one may estimate a global heat transfer coefficient in a heat exchanger from the steady-state heat balance of the system coupled with the classical DTLM model. Another way is to perform transient-state experiments and to estimate the heat exchange coefficient by using a dynamical model of the system and a parameter estimation technique.

In both cases, one may assume that the measured global heat exchange coefficient is sufficient to represent the heat transfer between the fluid and the wall: we adopt that assumption here.

The transient-state techniques have been widely used to measure heat exchange coefficients for different geometries and for gases and liquids. The principle of such techniques is to induce a transient state in a process comprising a fluid flowing through a solid system at a constant flow rate. To induce such a transient state, one uses the inlet fluid temperature or the solid wall temperature, and measures a fluid (generally the outlet one) or a solid temperature. The nature of the input signal is also variable, but impulse, step and frequency responses are mainly employed. Finally, these techniques have been used to study two categories of systems: heat exchangers and packed beds.

Transient test techniques are generally quick and easy to work, mainly because one only needs one fluid circuit. Furthermore, they are performed under nearly isothermal conditions and the power requirements are small because only small temperature changes are required. In the case of packed beds, another decisive advantage is that the solid surface temperature does not need to be measured.

Most of these methods are global input–output

† LAGEP-Université Lyon I-CPE URA CNRS D1328, 69622 Villeurbanne cedex, France.

NOMENCLATURE

A	section area [m^2]
a	thermal diffusivity [$m^2\ s^{-1}$]
C	inert tracer concentration [$mol\ m^{-3}$]
C_p	specific heat capacity [$J\ kg^{-1}\ K^{-1}$]
d	hydraulic diameter [m]
D	minimization criteria
e	solid wall thickness [m]
E	flow model transfer function
f	friction factor
G	global thermal model transfer function
h	heat exchange coefficient [$W\ m^{-2}\ K^{-1}$]
Im	imaginary part of a complex number
j	purely imaginary number, $j^2 = -1$
J	number of CSTRs
k	parameter in the friction factor equation
L	plate length [m]
l	plug flow reactor length [m]
M	local thermal model transfer function or mass [dimensionless or kg]
m	impulse response of the local thermal model
$\dot{m}$	specific mass flow rate [$kg\ s^{-1}\ m^{-2}$]
P	pressure [Pa]
q	volumic or mass flow rate [$m^3\ s^{-1}$ or $kg\ s^{-1}$]
Re, Re	Reynolds number or real part of a complex number
s	Laplace variable [s^{-1}]
t	time [s]
T	dead time corresponding to a plug flow reactor or temperature [s or K]
u	fluid velocity [$m\ s^{-1}$]
V	volume [m^3]
W	sensitivity parameters set
x	axial coordinate [m]
y	transversal coordinate [m].

Greek symbols

α	capacity factor
Δ	channel roughness [m]
ε	void fraction
Λ	dimensionless conduction parameter
λ	thermal conductivity [$W\ m^{-1}\ K^{-1}$]
μ	first-order moment of the local thermal model impulse response or dynamic viscosity [s or $kg\ m^{-1}\ s^{-1}$]
ρ	mass density [$kg\ m^{-3}$]
τ	first-order time constant corresponding to a CSTR or tortuosity factor [s or dimensionless]
ω	pulsation [$rad\ s^{-1}$].

Subscripts

cstr	continuous stirred tank reactor
exp	experimental
f	fluid
i	inlet
k	kth CSTR index
m	mass flow rate
n	nth measurement
o	outlet
pfr	plug flow reactor
s	solid wall
theo	theoretical
v	volumic flow rate
0	plug flow reactor index.

Superscripts

$\bar{T}$	spatial mean value of T
$'$	related to the entire heat exchanger.

methods based on inlet and outlet fluid temperature measurements. The so called 'single-blow transient test technique' is then based on the step response of the system. It has been widely used to measure the heat transfer coefficient between gases and heat exchanger surfaces [3–6]. Such step responses were also employed to measure heat transfer coefficient in packed beds [7, 8]. Frequency response has also been used to study packed or fluidized beds [9–14]. In some papers, authors propose estimating simultaneously up to three parameters, like the heat exchange coefficient, the fluid dispersion coefficient and the thermal conductivity of the solid packing [10–14]. Such multiple-parameter estimation has also been practised for heat exchangers area [15].

On the contrary, local methods are based on temperature measurements inside or along the system. For example, in ref. [16], the inside heat exchange coefficient between gas flow and a tube wall is estimated from the impulse response obtained by sudden heat generation inside the tube. The gas and external wall temperatures are then measured along the tube during cooling. One can also measure these temperatures at only one point on the tube, the transient state being obtained by the fluid inlet temperature oscillations [17] or the wall temperature oscillations [18].

All these methods need a model of the system. The physical properties of the fluid and the solid are generally considered to be constant; the flow rate being kept constant, these models are linear. The fluid flow is assumed to be a plug flow with or without axial dispersion while heat conduction in the solid is sometimes neglected. If some simplifications are not justified, errors will then occur in the estimation of the heat exchange coefficient [3, 19, 20]. It is particularly well known that axial dispersion in a fluid cannot be neglected at low Reynolds number [14, 20]. The data reduction method is also of great importance: it must be sensitive to the heat transfer coefficient. Many techniques have been used: a simple graphical exploitation of the step response like the maximum slope method [3], calculation of some function of the response based on its moments [21] and more sophisticated least-squares methods [6]. One will find a comparative study of these different techniques in ref. [22].

In this paper, we propose a global input–output method to measure the heat transfer coefficient between two parallel corrugated plates and a liquid flow. These corrugated plates are used for compact heat exchangers. In our model, we consider the fluid axial dispersion thanks to an equivalent flow pattern of the actual fluid flow. The latter is obtained from tracer experiments leading to the well-known residence time distribution (RTD) (see, for example, ref. [23]). Combined with a heat transfer model including the solid wall, this equivalent flow pattern gives the thermal model of the system: an experimental frequency response study leads to the estimation of the heat transfer coefficient by means of a least squares optimization method. This approach has already been used for packed [24] or fluidized beds [25] but, as far as we know, never for heat exchangers.

TRANSIENT-STATE MATHEMATICAL MODELLING

A sketch of the heat exchanger section is shown in Fig. 1. Two isolated corrugated plates, between which the liquid flows (water in our case), forming what we call the heat exchange section, are connected to the tubes of the external circuit by two inlet and outlet adaptation sections.

We plan to model transient heat transfer taking place between the corrugated plates and the fluid. Figure 2 shows a simplified scheme of the heat exchange section. The principle of our model is to assimilate the liquid flow to an equivalent flow pattern made of plug flows and perfectly mixed tanks [the classical PFR (plug flow reactor) and CSTR (continuous stirred tank reactor), both used to model flows through chemical reactors [23]]. The transient heat transfer is then modelled on the basis of this flow pattern.

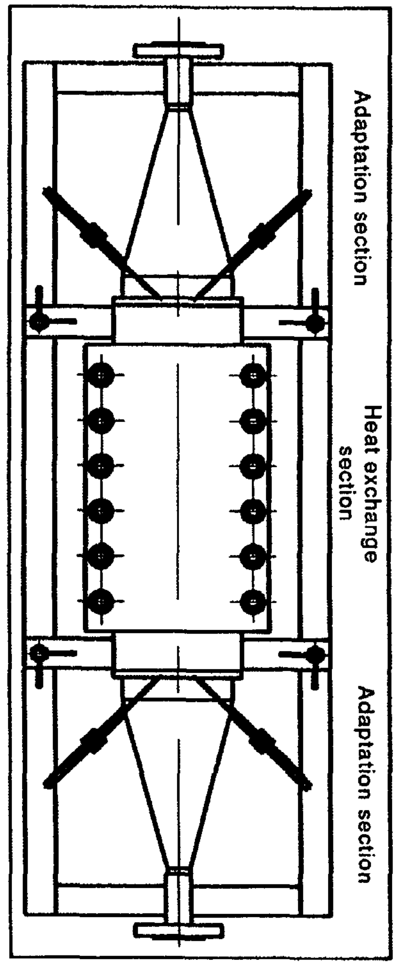

Fig. 1. Heat exchanger.

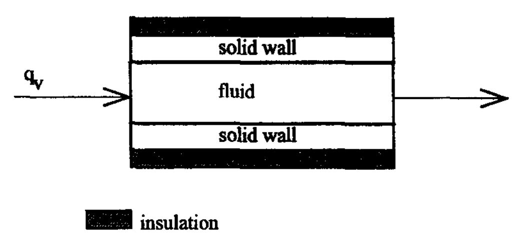

Fig. 2. Simplified scheme of the heat exchanger section.

Flow modelling

Figure 3 gives an example of such an equivalent pattern, modelling the flow with a serial arrangement of one PFR of volume V_0 and J identical CSTRs of volume V_k. Such an arrangement, which will be proved to fit our experimental results (see below), is obtained by measuring the outlet concentration of an inert tracer after its sudden introduction into the system. This curve, in fact the impulse response of the flow, leads to the determination of the RTD of the fluid in the system. The equivalent flow pattern is then built in order to give the same RTD as the actual one.

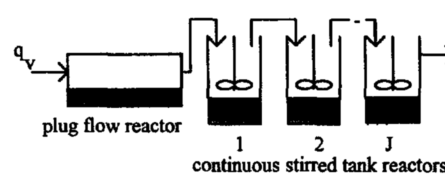

Fig. 3. Example of flow pattern.

The transfer function of a given flow pattern is obtained by combining the transfer functions of the PFR, which correspond to a dead time $E_0(s) = e^{-T_0 s}$, and of the CSTR, which corresponds to a first-order lag, $E_k(s) = 1/1+\tau_k s$. In the case of the flow pattern shown in Fig. 3, one can easily derive the following transfer function:

$$E(s) = \frac{e^{-T_0 s}}{(1+\tau_k S)^J} \quad \text{with}$$

$$T_0 = \frac{V_0}{q_v} \quad \text{and} \quad \tau_k = \frac{V_k}{q_v}. \tag{1}$$

The total volume of the flow V being constant, the following relation between the volumes of all the elements of the pattern must be verified:

$$V = \sum_{k=0}^{k=J} V_k. \tag{2}$$

$E(s)$ gives the dynamic relation between the outlet tracer concentration and the inlet one, $E(s) = C_o(s)/C_i(s)$. If no heat transfer occurs between the fluid and the solid wall, $E(s)$ also equals $T_o(s)/T_i(s)$, where T_i and T_o are, respectively, the fluid inlet and outlet temperatures.

TRANSIENT HEAT TRANSFER MODELLING

Hypothesis

Our model is based on the following assumptions:

- the axial dispersion in the fluid is considered by means of the equivalent flow pattern described above, and particularly the CSTR cascade;
- the heat transfer through the solid is supposed to be mainly transversal, as shown in Fig. 5. To justify such a hypothesis, we have computed the dimensionless parameter $\Lambda = (\lambda_s A_s)/(q_m C_{pf} L)$ for $0.239 \leqslant q_m \leqslant 0.480$ kg s^{-1}, the mass flow rate range that we have studied. We found $0.937 \times 10^{-5} \leqslant \Lambda \leqslant 1.882 \times 10^{-5}$, which seems to be negligible (see for example refs. [3] or [27]).

The second assumption is similar to that considered to model heat or mass transfer in packed beds (see, for example refs. [20] and [26]). In fact, the flow through our system is very close to the flow through a porous matrix, due to the extreme compactness of the heat exchange channel.

There are at least two lots of evidence for such a comparison:

(1) The void fraction ε is equal to 0.5, which is a value very close to that encountered for packed beds.

(2) One of us, Grillot [28], has measured the pressure drop ΔP of a gas flow between the same corrugated plates that we use here: Fig. 4 gives the evolution of $(\bar{\rho}\,\Delta P)/(L\mu\dot{m})$ vs $\dot{m}/\mu$. It can be seen that this curve is linear, except for the higher values of $\dot{m}/\mu$.

This pressure drop behaviour is similar to that observed in the case of flow through porous media. For example, in ref. [29] six regimes of such flows through packed beds of spheres are described according to the Reynolds number: respectively pre-Darcy flow, Darcy flow, the transition from Darcy to Forchheimer flow, Forchheimer flow, the transition from Forchheimer to turbulent flow, and, finally, turbulent flow. The first linear part of the curve in Fig. 4 corresponds to Forchheimer flow, also studied by Ergun [30]. For higher values of $\dot{m}/\mu$, we observe the transition to turbulent flow.

Many expressions similar to that of Ergun have been proposed to model Forchheimer flow. For example, an expression of $\Delta P/L$ is proposed in ref. [31], leading to the following expression of the friction factor f [28]:

$$f = \frac{16\gamma\tau^2}{Re} + 2k\tau^3. \tag{3}$$

From the experimental results shown in Fig. 4, Grillot [28] found $\tau = 2$ and $k = 0.0461$ with $\gamma = 1.22$. If, as according to Comiti and Renaud [31], we accept assimilation of k with the friction factor given by the Nikuradse formula for the completely rough flow regime, then

$$\frac{1}{\sqrt{\frac{k}{2}}} = 2.46 \ln\left(\frac{d}{2\Delta}\right) + 4.92. \tag{4}$$

We find that the roughness Δ of our channel is equal to 4.3 mm. This value corresponds approximately to the corrugation amplitude, and the value of the tortuosity factor ($\tau = 2$) indicates that the distance covered by the fluid is twice as long as the channel length, which is also a good approximation.

Let us now consider the heat transfer model of the PFR and CSTR elements of the equivalent flow pattern.

PFRs and CSTRs transient heat transfer modelling

Let $\bar{T}_s(x,t)$ and $T(x,t)$ be the mean solid temperature and the fluid temperature along the solid wall, respectively. From the solid and fluid heat balance, one can derive the following equation:

$$u\frac{\partial T}{\partial x} + \alpha\frac{\partial \bar{T}_s}{\partial t} + \frac{\partial T}{\partial t} = 0 \quad \text{with} \quad \alpha = \frac{M_s C_{ps}}{M_f C_{pf}}. \tag{5}$$

α is the ratio of the plate heat capacity to that of the fluid present in the channel.

By taking the Laplace transform of equation (5), defining the local transfer function

$$M(s) = \frac{\bar{T}_s(x,s)}{T(x,s)}$$

the inlet–outlet fluid temperature transfer function then occurs, after integration between the PFR inlet $x = 0$ and outlet $x = l$:

$$G_0(s) = \frac{T_{pfr,o}}{T_{pfr,i}} = e^{-T_0 s(1+\alpha M(s))} \quad \text{with } T_0 = \frac{l}{u} = \frac{V_0}{q_v}. \tag{6}$$

In the case of the CSTR, the fluid temperature is only time-dependent and the corresponding heat balance leads to

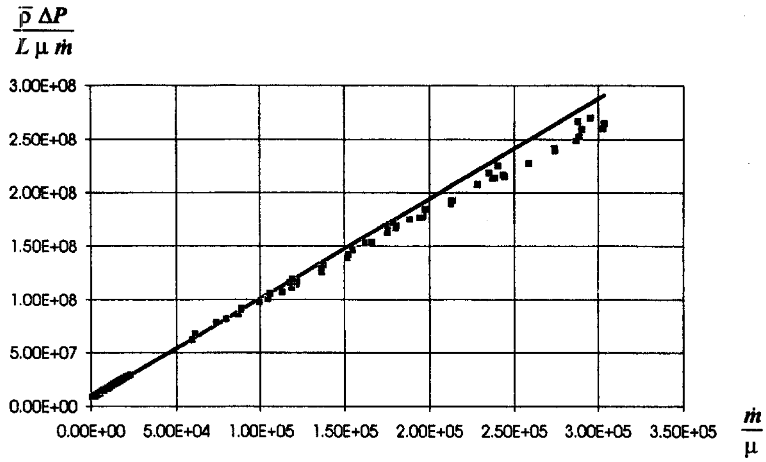

Fig. 4. $(\bar{p}\Delta P)/(L\mu\dot{m})$ vs $\dot{m}/\mu$ for a gas flow between the same corrugated plates.

$$\tau_k \frac{\mathrm{d}T_{\mathrm{cstr,o}}}{\mathrm{d}t} + \alpha\,\tau_k \frac{\mathrm{d}\bar{T}_{\mathrm{s}}}{\mathrm{d}t} + T_{\mathrm{cstr,o}} = T_{\mathrm{cstr,i}}. \quad (7)$$

The transfer function then, is the following:

$$G_k(s) = \frac{1}{1+\tau_k s\,(1+\alpha M(s))}. \quad (8)$$

Local transient heat transfer modelling: M(s) *derivation*

Figure 5 gives a schematic view of a wall section at an arbitrary axial coordinate x. At $y = 0$, the wall is in contact with the fluid at a temperature T, the fluid–solid heat exchange coefficient being h, and, at $y = e$, the wall is supposed to be perfectly insulated.

The solid temperature $T_s(y, t)$ is then the solution of the following equation:

$$a\frac{\partial^2 T_s}{\partial y^2} = \frac{\partial T_s}{\partial t}$$

with

$$\left(\frac{\partial T_s}{\partial y}\right)_{y=e} = 0 \quad \text{and} \quad -\lambda_s\left(\frac{\partial T_s}{\partial y}\right)_{y=0} = h\,(T - T_s). \quad (9)$$

By using the Laplace transform technique, one can derive the following expression of the local transfer function:

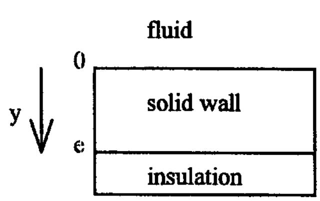

Fig. 5. Local heat transfer modelling.

$$M(s) = \frac{\bar{T}_s(s)}{T(s)}$$

$$= \frac{e^{\sqrt{\frac{s}{a}}e} - e^{-\sqrt{\frac{s}{a}}e}}{\sqrt{\frac{s}{a}}\,e\left[\left(1+\frac{\lambda_s}{h}\sqrt{\frac{s}{a}}\right)e^{\sqrt{\frac{s}{a}}e} + \left(1-\frac{\lambda_s}{h}\sqrt{\frac{s}{a}}\right)e^{-\sqrt{\frac{s}{a}}e}\right]} \quad (10)$$

where

$$\bar{T}_s(t)e = \int_0^e T_s(y, t)\,\mathrm{d}y$$

is the mean spatial solid temperature.

From equation (10), one can derive the expression of the first order moment of the impulse response $m(t)$ corresponding to $M(s)$ defined by

$$\mu = \int_0^\infty t m(t)\,\mathrm{d}t$$

i.e.

$$\mu = -\left(\frac{\partial M(s)}{\partial s}\right)_{s=0} = \frac{e^2}{4a} + \frac{\rho_s C_{ps}\,e}{h}. \quad (11)$$

The second term of this relation is the first moment of $m(t)$ if heat conduction in the solid is negligible. In our case, $e^2/4a$ is very small compared to $(\rho_s C_{ps} e)/h$, and we assume here that the solid temperature is homogeneous, i.e.

$$M(s) \approx \frac{1}{1+\mu s}. \quad (12)$$

Inlet–outlet modelling of the heat exchanger channel

By combining the transfer functions described above according to a serial arrangement of one PFR and J identical CSTRs (see Fig. 3), the global transfer

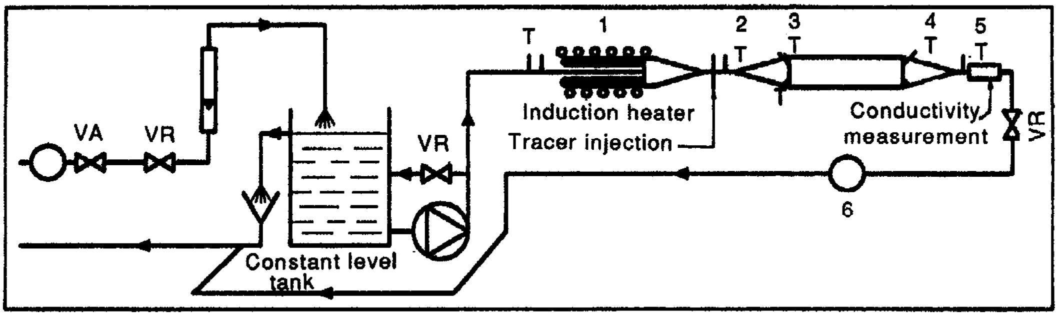

Fig. 6. Schematic view of the experimental set-up.

function between the fluid outlet and inlet temperatures is

$$G(s) = \frac{e^{-T_0 s(1+\alpha M(s))}}{[1+\tau_k s(1+\alpha M(s))]^J}. \tag{13}$$

It is well known that the frequency response of such a linear system is simply given by the complex number $G(s = j\omega)$.

Finally, one must notice the similarity between the two transfer functions (1) and (13): $G(s)$ [equation (13)] is obtained by replacing s with $s(1+\alpha M(s))$ in $E(s)$ [equation (1)].

This is in fact a particular application of a general theorem [32], allowing the modelling of linear percolation processes through constant void fraction porous media.

The flow is characterized by its RTD and can also be represented by a parallel arrangement of an infinity of elementary PFRs, of which residence time is distributed according the experimental RTD. On this basis, one can associate a solid volume with each of the elementary PFRs, according to the global fluid–solid mass repartition [see the capacity factor definition in equation (5)], leading to an input–output model similar to that derived for our system.

EXPERIMENTAL SET-UP

Figure 6 shows a schematic view of the experimental apparatus. The plates are made of stainless steel, Table 1 gives the mains characteristics of the system.

The fluid inlet temperature oscillations are obtained by using an induction heating system **1**. This system generates Foucault currents in a ferromagnetic steel element, and consequently heat by the Joule effect. A high Reynolds number fluid flow around this element leads to a high heat exchange coefficient. A tension modulation allows temperature oscillations of frequency between 0.1 and 1.0 Hz.

Table 1. Main characteristics of the heat exchanger

Plate thickness	0.0007 m
Plate width	0.133 m
Plate length	0.396 m
Heat exchange area	0.1253 m^2
Inlet section area	0.0005 m^2
Fluid volume between the plates	0.27×10^{-3} m^3
Corrugation amplitude	0.0039 m
Corrugation period	0.013 m
Corrugation angle	60°

The fluid temperatures are measured at the inlet and the outlet of the heat exchanger (**2** and **5**) and of the heat exchange section itself (**3** and **4**). We used 0.25 mm diameter K thermocouples, directly in contact with the fluid. The time constant of such sensors is about 0.01 s, which is negligible. The inert tracer (an NaCl saturated solution) is injected at the inlet of the heat exchanger **2**, from a pressurized tank. The injection time is controlled by an electrovalve. Conductivity measurements give the evolution of the tracer concentration at the outlet **5**. The flow rate is measured with an electromagnetic flow meter **6**.

RESULTS AND DISCUSSION

We did three experiments for three values of the Reynolds number, $Re = 3100$, 4690 and 6240, respectively. As an example, we show in Figs. 7 and 8 the RTD and the frequency response for $Re = 6240$. The frequency response is plotted in the Nyquist diagram which means Im $(G(j\omega))$ vs Re $(G(j\omega))$.

We recall that the RTD measurements are related to the entire heat exchanger, between points **2** and **5**, while the frequency response is measured between points **3** and **4** (see Fig. 6). In order to estimate the heat exchange coefficient, we planned to fit simultaneously our model to both the experimental RTD and the frequency response. The schedule for this procedure is the following:

- *step* 1—heat exchanger flow modelling between points **2** and **5**. It consists of the direct measurement of the total dead time T_0' and the estimation of the number of CSTRs and their volume, in order to minimize

$$D = \sum_n (E'(t_n)_{\text{exp}} - E'(t_n)_{\text{theo}})^2$$

- *step* 2—heat exchange channel flow modelling

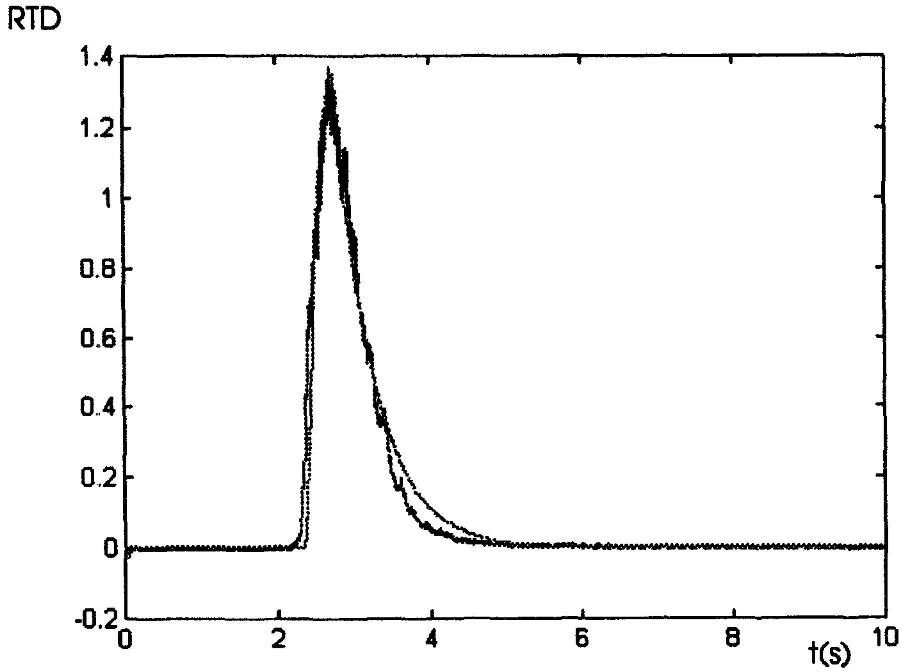

Fig. 7. Experimental and theoretical RTDs for $Re = 6240$.

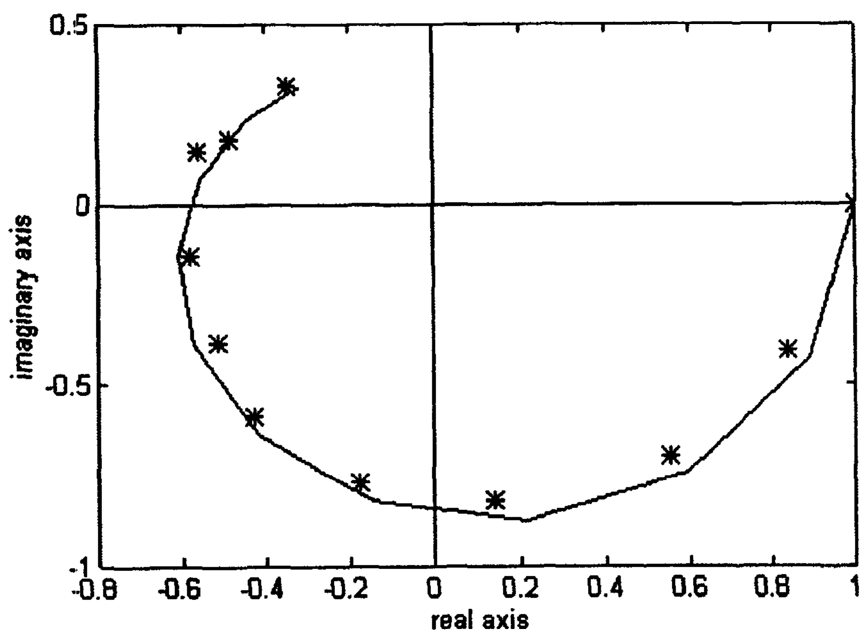

Fig. 8. Experimental and theoretical frequency responses for $Re = 6240$.

between points 3 and 4. We extract the flow pattern corresponding to this subsystem in order to respect the total volume constraint [relation (2)] of this section and to qualitatively fit its experimental frequency response;

- *step* 3—heat exchange coefficient estimation. We obtain h by minimizing the following criteria

$$D = \sum_n W(\omega_n)\,[\mathrm{Re}\,(G(j\omega_n)_{\mathrm{exp}}) - \mathrm{Re}\,(G(j\omega_n)_{\mathrm{theo}})]^2 + [\mathrm{Im}\,(G(j\omega_n)_{\mathrm{exp}}) - \mathrm{Im}\,(G(j\omega_n)_{\mathrm{theo}})]^2.$$

$W(\omega_n)$ is a set of sensitivity parameters arbitrarily

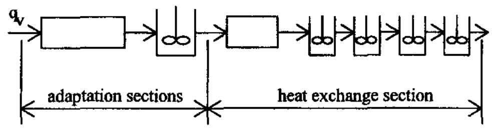

Fig. 9. Equivalent flow pattern of the heat exchanger.

Table 2. Comparison of our results with previous work [33]

Reynolds number	h [W m^2 K^{-1}] Our results	h [W m^2 K^{-1}] [33]	Error [%]
3100	13 670	13 910	2
4790	18 970	18 620	2
6240	23 850	22 770	5

defined from a sensitivity study of the frequency response to h.

Figures 7 and 8 show that our model correctly fits the experimental results. The corresponding flow modelling is shown in Fig. 9. The heat exchange section is equivalent to one PFR of volume $V_0 = 160\,\text{cm}^3$ and four identical CSTRs of volume $V_k = 28\ \text{cm}^3$, while the two adaptation sections are equivalent to one PFR of volume $V'_0 = 940\,\text{cm}^3$ and one CSTR of volume $V'_1 = 250\,\text{cm}^3$.

The equivalent flow pattern of the heat exchange section has proved to be constant in our range of Reynolds number.

Table 2 shows a comparison between our results and those already known for such corrugated plates [33].

We can see that these results are not significantly different.

Remark: the theoretical curves shown here are calculated by using the Matlab Software (The Math Works, Inc., U.S.A.) on a personal computer.

CONCLUSION

In many circumstances, transient-state techniques have proved their efficiency in order to measure heat transfer coefficients in packed beds or heat exchangers. The lack of accuracy that has sometimes been recorded is mainly due to model inadequacy, particularly in the case of low Reynolds numbers when axial dispersion is neglected in the fluid.

In this paper, we use simultaneously two independent transient-state techniques. RTD measurement gives an equivalent flow pattern model of the flow, allowing the fluid axial dispersion modelling. The heat transfer model is then based on this equivalent flow pattern, the frequency response leading to the global heat transfer coefficient.

This general framework of analysis is adapted to systems in which the flow can be assimilated to a flow through a porous matrix; in this case, one can associate an amount of solid in the same ratio as that of the system to each element of the equivalent flow pattern. We give some evidence based on pressure drop measurements that our system can be compared with a flow through a porous matrix.

Finally, as far as mathematical treatments are concerned, we want to emphasize here the advantage of frequency analysis, which transforms the ordinary or partial differential equation resolution into simple algebraic computations. Even if experimental frequency analysis is not performed, in consideration of technical difficulties, one can use non-parametric estimation procedures based on Fourier transform. Particularly, the frequential representation of systems facilitates the sensitivity analysis of the measured variable to the estimated parameters. Such an analysis is necessary to design a transient-state measurement method.

REFERENCES

1. D. Petit, J. Dard and A. Degiovanni, Détermination du coefficient d'échange entre un fluide et une paroi, *Rev. Gén. Therm. Fr.* **238,** 719–732 (1981).
2. P. Pierson and J. Padet, Evaluation des transferts thermoconvectifs en régime instationnaire. Approche théorique et expérimentale, *Rev. Gén. Therm. Fr.* **287,** 781–788 (1985).
3. P. F. Pucci, C. P. Howard and C. H. Piersall Jr, The single-blow transient testing technique for compact heat exchanger surfaces, *Trans. ASME J. Engng Power* **89,** 29–40 (1967).
4. C. Y. Liang and W. J. Yang, Modified single-blow technique for the performance evaluation on heat transfer surfaces, *Trans. ASME J. Heat Transfer* **97,** 16–21 (1975).
5. Z. H. Cai, M. L. Li, Y. W. Wu and H. S. Ren, A modified selected point matching technique for testing compact heat exchanger surfaces, *Int. J. Heat Mass Transfer* **27,** 971–978 (1984).
6. R. S. Mullisen and R. I. Loehrke, A transient heat exchanger evaluation test for arbitrary fluid inlet temperature variation and longitudinal core conduction, *Trans. ASME J. Heat Transfer* **108,** 370–376 (1986).
7. D. Handley and P. J. Heggs, Momentum and heat transfer mechanisms in regular shaped packings, *Trans. Instn Chem. Engrs* **46,** T251–T264 (1968).
8. A. V. Bradshaw, A. Johnson, N. H. McLachlan and Y.-T. Chiu, Heat transfer between air and nitrogen and packed beds of non-reacting solids, *Trans. Instn Chem. Engrs* **48,** T77–T84 (1970).
9. H. Littman, R. G. Barile and A. H. Pulsifer, Gas–particle heat transfer coefficients in packed beds at low Reynolds numbers, *Ind Engng Chem. Fundam.* **7,** 554–561 (1968).
10. G. C. Lindauer, Heat transfer in packed and fluidized beds by the method of cyclic temperature variations, *A.I.Ch.E. Jl* **13,** 1181–1187 (1967).
11. G. A. Turner, A method for finding simultaneously the values of the heat transfer coefficient, the dispersion coefficient, and the thermal conductivity of the packing in a packed bed of spheres, *A.I.Ch.E. Jl* **13,** 678–682 (1967).
12. G. A. Turner and L. Otten, Value of thermal (and other) parameters in packed beds, *Ind. Engng Chem. Process Des. Dev.* **12,** 417–424 (1973).
13. M. J. Goss and G. A. Turner, Simultaneous computation of heat transfer and dispersion coefficients and thermal conductivity value in a packed bed of spheres, *A.I.Ch.E. Jl* **17,** 590–595 (1971).
14. D. J. Gunn and J. F. C. De Souza, Heat transfer and axial dispersion in packed beds, *Chem. Engng Sci.* **29,** 1363–1371 (1974).

15. W. Roetzel, X. Luo and Y. Xuan, In *Proceedings of the Third World Conference on Experimental Heat Transfer, Fluid Mechanics and Thermodynamics* (Edited by M. D. Kelleher *et al.*), Vol. 1, pp. 180–186. Elsevier, Amsterdam (1993).
16. A. Massaad, J. Dard, Ph. Gervais and M. Laurent, Coefficients d'échange dans une conduite cylindrique. Evaluation expérimentale, *Rev. Gén. Therm. Fr.* **286,** 731–737 (1985).
17. W. Roetzel, Measurement of heat transfer coefficients in tubes by temperature oscillation analysis, *Chem. Engng Technol.* **12,** 379–387 (1989).
18. F. Mirtsch and W. Roetzel, Measuring local heat transfer coefficients on profiled walls of heat exchangers, *Proceedings of the International Symposium on New Developments in Heat Exchangers*, p. 2.1. Lisbonne (1993).
19. R. I. Loehrke, Evaluating the results of the single-blow transient heat exchanger test, *Expl. Therm. Fluid Sci.* **3,** 574–580 (1990).
20. N. Wakao, S. Kaguei and T. Funazkri, Effect of fluid dispersion coefficients on particle-to-fluid heat transfer coefficients in packed beds, *Chem. Engng Sci.* **34,** 325–336 (1979).
21. G. F. Kohlmayr, An indirect curve matching method for transient matrix heat-transfer testing in the low N_{tu}-range, *Int. J. Heat Mass Transfer* **11,** 567–581 (1968).
22. P. J. Heggs and D. Burns, Single-blow experimental prediction of heat transfer coefficients. A comparison of four commonly used techniques, *Expl. Therm. Fluid Sci.* **1,** 243–251 (1988).
23. O. Levenspiel, *Chemical Reaction Engineering*. Wiley, New York (1962).
24. C. Roizard and D. Tondeur, Comportement thermique d'un lit fixe traversé par un gaz. Expériences et modélisation, *Entropie* **125/126,** 60–72 (1985).
25. M. Tayakout and C. Jallut, Use of RTD and local transfer representation to obtain a transient modelling of a liquid–solid system, *Chem. Engng Commun.* **117,** 163–174 (1992).
26. V. Hlavacka, Periodic heating of a system of cylinders and determining the heat-transfer coefficient on this basis, *J. Engng Phys.* **24,** 52–55 (1973).
27. C. W. Rapley and A. I. C. Webb, Heat transfer performance of ceramic regenerator matrices with sine-duct shaped passages, *Int. J. Heat Mass Transfer* **26,** 805–814 (1983).
28. J. M. Grillot, Etude du dépôt de particules en phase gazeuse dans des canaux d'échangeurs thermiques, Ph. D. thesis, Institut National Polytechnique de Grenoble (1989).
29. R. M. Fand, B. Y. K. Kim, A. C. C. Lam and R. T. Phan, Resistance to the flow of fluids through simple and complex porous media whose matrices are composed of randomly packed spheres, *J. Fluid Engng* **109,** 268–274 (1987).
30. S. Ergun, Fluid flow through packed columns, *Chem. Engng Prog.* **48,** 98 (1952).
31. J. Comiti and M. Renaud, A new model for determining mean structure parameters of fixed beds from pressure drop measurements: application to beds packed with parallelepipedal particles, *Chem. Engng Sci.* **44,** 1539–1545 (1989).
32. J. Villermaux, Deformation of chromatographic peaks under the influence of mass transfer phenomena, *J. Chromat. Sci.* **12,** 822–831 (1974).
33. P. Hugonnot, Etude locale de l'écoulement et performances thermohydrauliques à faible nombre de Reynolds d'un canal plan corrugué—Applications aux échangeurs de chaleur à plaques, Ph.D. thesis, University of Nancy I (1989).